NEOPLASIA
www.neoplasia.com

Volume 12 Number 4 April 2010 pp. 336–345 336

# Pigment Epithelium–Derived Factor Stimulates Tumor Macrophage Recruitment and Is Downregulated by the Prostate Tumor Microenvironment[1]

**Sofia Halin*, Stina Häggström Rudolfsson†, Jennifer A. Doll‡, Susan E. Crawford‡, Pernilla Wikström* and Anders Bergh***

*Department of Medical Biosciences, Pathology, Umeå University, Umeå, Sweden; †Department of Surgical and Perioperative Sciences, Urology and Andrology, Umeå University, Umeå, Sweden; ‡Department of Surgery, NorthShore University HealthSystem Research Institute, Evanston, IL, USA

## Abstract

Pigment epithelium–derived factor (PEDF) is a potent inhibitor of angiogenesis but whether it has additional effects on the tumor microenvironment is largely unexplored. We show that overexpression of PEDF in orthotopic MatLyLu rat prostate tumors increased tumor macrophage recruitment. The fraction of macrophages expressing inducible nitric oxide synthase, a marker of cytotoxic M1 macrophages, was increased, suggesting that PEDF could enhance antitumor immunity. In addition, PEDF overexpression reduced vascular growth both in the tumor and in the surrounding normal tissue, slowed tumor growth, and decreased lymph node metastasis. Contrary, extratumoral lymphangiogenesis was increased. PEDF expression is, for reasons unknown, often decreased or lost during prostate tumor progression. When AT-1 rat prostate tumor cells, expressing high levels of PEDF messenger RNA (mRNA) and protein, were injected into the prostate, PEDF is markedly downregulated, suggesting that factors in the microenvironment suppressed its expression. One such factor could be macrophage-derived tumor necrosis factor α (TNFα). A fraction of the accumulating macrophages expressed TNFα, and TNFα treatment downregulated the expression of PEDF protein and mRNA in prostate AT-1 tumor cells *in vitro* and in the rat ventral prostate *in vivo*. PEDF apparently has multiple effects in prostate tumors: it suppresses angiogenesis and metastasis, but it also causes macrophage accumulation. Accumulating macrophages may inhibit tumor growth, but they may also suppress PEDF and enhance lymph angiogenesis and, in this way, eventually enhance tumor growth.

*Neoplasia (2010) 12, 336–345*

## Introduction

Prostate tumors contain, in addition to tumor epithelial cells, many different cancer-associated stromal cells, including cancer-associated fibroblasts, infiltrating immune cells and blood vessels. The cancer cells alter the stromal cells, activating them such that this microenvironment becomes largely tumor promoting [1]. Macrophages are the most abundant immune cells present in the tumor microenvironment [2]. Tumor-associated macrophages (TAMs) may have both tumor-stimulatory and/or -inhibitory properties, probably because they can, by mechanisms largely unknown, differentiate into either cytotoxic (M1) or tumor growth-promoting (M2) states. Classically, proinflammatory (M1) macrophages express inducible nitric oxide synthase (iNOS) in contrast to immunosuppressive (M2) macrophages [3].

Abbreviations: CCL2/MCP-1, monocyte chemoattractant protein 1; FGF2, fibroblast growth factor 2; GAPDH, glyceraldehyde-3-phosphate dehydrogenase; iNOS, inducible nitric oxide synthase; PEDF, pigment epithelium–derived factor; PlGF, placental growth factor; TAM, tumor-associated macrophage; TLR4, Toll-like receptor 4; TNFα, tumor necrosis factor α; VEGF, vascular endothelial growth factor

Address all correspondence to: Dr. Sofia Halin or Prof. Anders Bergh, Department of Medical Biosciences, Pathology, Umeå University, S-90187 Umeå, Sweden.
E-mail: sofia.halin@medbio.umu.se or anders.bergh@medbio.umu.se

[1]This work was supported by the Swedish Cancer Society, the Swedish Research Concil, the University Hospital of Northern Sweden, and the Lions Cancer Research Foundation, Umeå University.
Received 17 December 2009; Revised 8 February 2010; Accepted 8 February 2010


DOI 10.1593/neo.92046

TAMs generally exhibit an M2 phenotype known to promote angiogenesis, tumor growth, and metastasis [3,4].

In prostate cancer, the significance of macrophage infiltration is unclear. In one study, the presence of macrophages was associated with angiogenesis and poor outcome [5], but another study reported no association [6]. A study in mice showed that inhibition of the macrophage chemoattractant, monocyte chemoattractant protein 1 (MCP-1; also called CCL2), in a prostate xenograft model reduced macrophage infiltration, angiogenesis, and tumor growth [7]. We have previously shown that an overall reduction of monocyte/macrophage recruitment to orthotopic rat prostate tumors represses tumor growth and angiogenesis both in the tumor and in the surrounding nonmalignant tissue [8]. However, none of these studies distinguished between M1 and M2 TAM subtypes.

Pigment epithelium–derived factor (PEDF), a 50-kDa secreted glycoprotein with multifunctional properties, has also been implicated in both proinflammatory and anti-inflammatory processes in neuronal tissues and in the eye [9–13]; however, its role in tumor inflammation is unknown. PEDF also functions in neuronal cell survival and differentiation [14] and has potent antiangiogenic activity [15]. Owing to its antiangiogenic properties, the potential antitumor activity of PEDF has been investigated. To date, a number of studies have demonstrated that PEDF represses tumor growth and suppresses metastasis in several types of cancers [16–22]. The antitumor effects of PEDF include both indirect actions through inhibition of angiogenesis and direct inhibition of tumor cell migration, induction of apoptosis, and differentiation [23–25].

In prostate cancer, treatment of subcutaneous prostate xenografts with recombinant PEDF protein inhibited angiogenesis and increased tumor necrosis [26]. Treatments with different PEDF epitopes have also shown to inhibit growth of experimental prostate tumors either through antiangiogenic effects or by inducing neuroendocrine differentiation [27]. We have earlier shown that decreased PEDF levels are associated with a higher vascular density and a metastatic phenotype in both human and rat prostate tumors [28]. An inverse correlation among PEDF levels, grade, and metastatic potential has also been seen for several other tumors, indicating that PEDF expression is decreased during tumor progression [29–34].

The underlying mechanisms for decreased PEDF expression in tumors are unknown but could be due to genetic or epigenetic changes. Regulatory signals from the microenvironment may also influence PEDF expression. Hypoxia and androgens have, for instance, been shown to downregulate PEDF in prostate tumors [26].

In this study, MatLyLu rat prostate tumor cells transfected to overexpress human PEDF were examined for tumor growth, angiogenesis, lymphangiogenesis, metastasis, and tumor macrophage infiltration. Furthermore, we examined prostate environmental regulation of PEDF in rat prostate tumors.

Consistent with previous studies, the current study shows that PEDF overexpression suppresses orthotopic rat prostate tumor growth, angiogenesis, and metastasis, although it increased extratumoral lymphangiogenesis. We also show that endogenous PEDF is downregulated by the prostate microenvironment. We demonstrate that this downregulation is likely due in part to macrophage-derived tumor necrosis factor α (TNFα) because TNFα down-regulated PEDF expression in prostate tumor cells *in vitro* and in the ventral prostate *in vivo*. In addition, we show that PEDF increased tumor macrophage infiltration and increased the fraction of iNOS-positive TAMs in the tumors, suggesting an increase in tumoricidal M1 macrophage activity.

## Materials and Methods

### *Cell Culture*

Tumor cell lines (ATCC, LGC Standards, Borås, Sweden) were grown in RPMI 1640 with 10% fetal calf serum, 0.2% Na-Bic, 50 μg/ml gentamicin, and 250 nM dexamethasone in 37°C and 5% $CO_2$. Human umbilical vein endothelial cells (Cascade Biologics, Paisley, UK) were grown in Medium 200 (Cascade Biologics) supplemented with low serum growth supplement (Cascade Biologics). Serum-free conditioned medium was collected as described previously [26,28].

### *Transfection of PEDF into MatLyLu Rat Prostate Tumor Cells*

The human PEDF complementary DNA (cDNA) cloned into a pCEP4 construct [15] was used for transfection of MatLyLu rat prostate tumor cells. Cells were transfected with Lipofectamine (Invitrogen, Stockholm, Sweden) according to the manufacturer's instruction. MatLyLu cells transfected with pCEP4 empty plasmid vector (Invitrogen) were used as controls. Transfected cells were selected using Hygromycin B (Invitrogen). The expression of PEDF was confirmed by Western blot.

### *3-(4,5-Dimethylthiazol-2-yl)-2,5 diphenyltetra-zolium Bromide Viability Assay*

Viability was determined by the 3-(4,5-dimethylthiazol-2-yl)-2,5 diphenyltetra-zolium bromide (MTT) assay (Roche Diagnostics, Bromma, Sweden). Briefly, PEDF transfected cells (MatLyLu-PEDF) or control cells (MatLyLu-CON) (10,000 cells per well) were seeded in 100 μl in a 96-well plate and incubated in 37°C. After 72 hours, 10 μl of MTT labeling reagent was added to each well and incubated for an additional 4 hours. Then, 100 μl of solubilization solution was added into each well and incubated overnight. The following day, absorbance was measured at 550 nm and subtracted with the reference wavelength at 650 nm.

### In Vitro *Angiogenesis Assay*

For PEDF protein purification, conditioned media from MatLyLu-PEDF transfected cells was purified on a HisTrap HP column according to the manufacturer's instructions (Novagen, Darmstadt, Germany). The eluted sample was dialyzed against PBS using a dialysis cassette with 10-kDa cutoff (Pierce Chemical Co, Rockford, IL). Purification of PEDF protein was determined by Coomassie-stained SDS-polyacrylamide gels and Western blot (results not shown).

HUVEC endothelial cell migration was studied in modified Boyden chambers containing chemotaxis membranes with an 8-μm pore size (Neuroprobe, Gaithersburg, MD) which were coated with Collagen 1 (Cohesion, Palo Alto, CA). Cells were washed and detached by trypsinization and resuspended in serum-free medium containing 0.1% BSA. Approximately 10,000 cells were seeded in the top wells. Serum-free medium with 0.1% BSA containing test substances were placed in the lower chambers. After incubation for 6 hours at 37°C, filters were fixed and stained with Giemsa and mounted. Cells attached to the bottom side of the membrane were counted visually under the microscope (three high-power fields per well). Six wells per test substance were assayed, and data were confirmed by two independent experiments. Serum-free medium containing 0.1% BSA served as a control for background migration, and fibroblast growth factor 2 (FGF2) (10 ng/ml; Peprotech, Rocky Hill, NJ) served as a positive control. Purified PEDF (0.1 μg/ml) alone or in combination with FGF2 was tested. Results were presented as a percent of the maximal migration toward the positive control after subtracting the background migration.

### *Animal Studies*

MatLyLu-PEDF or MatLyLu-CON cells (10,000 cells in 50 μl of RPMI) were carefully injected into the ventral prostate of Copenhagen rats as previously described [35]. Animals were killed at 7 (MatLyLu-PEDF, $n = 7$; MatLyLu-CON, $n = 8$) and 23 days (MatLyLu-PEDF, $n = 11$; MatLyLu-CON, $n = 9$) after tumor cell injection. At sacrifice, the animals were injected with bromodeoxyuridine (BrdU, 50 mg/kg; Sigma-Aldrich, Oslo, Norway) and anesthetized 1 hour later. The tumor, liver, regional lymph nodes, and lungs were removed, weighed, fixed in 4% paraformaldehyde, dehydrated, and paraffin-embedded before morphologic analysis.

AT-1 (2000 cells in 50 μl RPMI, $n = 5$) were injected into the ventral prostate of Copenhagen rats as previously described [8]. Animals were killed at day 10, and tumors were quickly removed, frozen in liquid nitrogen, and stored at −80°C. Frozen AT-1 tumor tissue was carefully dissected before protein and RNA extraction. For immunohistochemistry staining, the AT-1 tumors were removed, formalin-fixed, and prepared as earlier described [35].

All the animal work was approved by the local ethical committee for animal research.

### *Immunohistochemistry and Morphologic Analyses*

Tissue sections were deparaffinized, rehydrated, and washed according to standard procedures. Immunohistochemical staining was performed using primary antibodies against human PEDF (1:100, cat. MAB1059; Chemicon, Temecula, CA), rat TNFα (1:1000, cat. AAR33; AbD Serotec, Oxford, UK), synaptophysin (1:100, cat. A0010; Dako, Stockholm, Sweden), LYVE-1 (1:100, cat. Ab14917; Abcam, Cambridge, UK), or iNOS (1:500, cat. Ab15323; Abcam) incubated overnight. After incubating with secondary antibodies, the slides were then developed using diaminobenzidine (Dako).

Five-micrometer-thick sections were immunostained using primary antibodies against factor VIII (Dako), BrdU (Dako), caspase-3 (Cell Signaling Technology, Danvers, MA), and CD68 (AbD Serotec) as described earlier [36–38]. The volume densities (percentages of tissue volume occupied by the defined tissue compartment) of factor VIII–stained blood vessels, LYVE-1–positive lymph vessels, CD68-positive macrophages, and iNOS-positive macrophages were assessed by a point cutting method as earlier described [36,38]. Briefly, a 121-point square lattice mounted in the eyepiece of a light microscope was used to count the number of intersections falling on the respective compartment and reference tissue in randomly chosen fields. The fraction (%) of BrdU-positive proliferating tumor cells and apoptotic caspase-3–positive tumor cells were measured in approximately 500 cells in each animal as described earlier [36,38]. Volume density of tumor tissue at day 7 was determined on hematoxylin-eosin–stained sections as previously described [35,36,38]. Total tumor weight was then estimated by multiplying the volume density with prostate weight. The size of lymph node metastasis was estimated by measuring the largest diameter of each metastasis.

### *TNFα Stimulation* In Vitro *and* In Vivo

AT-1 cells ($5 \times 10^5$) were seeded in 1 ml of complete medium in a 12-well plate and allowed to settle overnight. The cells were rinsed in PBS, incubated in serum-free medium for 4 hours, and washed. Rat recombinant TNFα (Sigma-Aldrich) diluted in serum-free medium was then added to the cells (1, 10, and 100 ng/ml, three wells per concentration) and incubated for 18 hours. Serum-free medium was used as controls (three wells). RNA was then prepared as described (see below). The results were confirmed in two independent experiments. For protein analysis, AT-1 cells were grown to approximately 70% to 80% confluence and then washed and incubated for 24 hours with TNFα (100 ng/ml) or control medium (0 ng/ml) in the same way as for RNA preparation. Serum-free conditioned medium was collected as described previously [26,28]. For *in vivo* studies, TNFα (1 μg in 10 μl of PBS, $n = 5$) or control solution (10 μl of PBS, $n = 5$) was injected into the ventral prostate of Copenhagen rats. The animals were killed after 6 hours, and the ventral prostates were quickly removed and frozen in liquid nitrogen before RNA extraction.

### *Protein Preparation and Western Blot*

Frozen AT-1 tumors were homogenized and transferred into a lysis buffer as previously described [28]. Protein extracts were then pooled together ($n = 3$). The BCA Protein Assay (Pierce) was used to determine the protein concentration.

Western blot was performed as previously described [28] using primary antibodies for PEDF ([15] for rat PEDF and Chemicon for human PEDF, at 1:1000, for 1 hour). Molecular-size standards (BioRad Laboratories AB, Hercules, CA) were included as controls.

### *RNA Preparation, RT$^2$ Profiler PCR Arrays, and Real-time Quantitative Reverse Transcription–Polymerase Chain Reaction*

RNA, from ventral prostate, AT-1 tumors ($n = 5$), AT-1 cells ($n = 3$ different cell batches), and MatLyLu-transfected cells, was extracted using the TRIzol method (Invitrogen) following the manufacturer's instructions.

For polymerase chain reaction (PCR) array studies, MatLyLu-PEDF cells ($n = 4$ different cell batches, pooled into one sample) were compared with MatLyLu-CON cells ($n = 4$ different cell batches, pooled into one sample). Total RNA was DNase-treated, and complementary DNA (cDNA) was synthesized on 1 μg as previously described [8]. RT$^2$ Profiler PCR arrays, rat angiogenesis (cat. APRN-024A; SABiosciences, Frederick, MD), and rat chemokines (cat. PARN-022A; SABiosciences) were performed and analyzed as previously described [8] and according to the manufacturer.

Quantification of PEDF mRNA levels was performed by real-time quantitative reverse transcription–PCR using the LightCycler SYBR Green I technology (Roche Diagnostics) as previously described and according to a protocol [28]. Melting curve analysis was performed to confirm specificity. Negative controls were run in parallel. Glyceraldehyde-3-phosphate dehydrogenase (GAPDH) mRNA was analyzed to control that equal levels of RNA were analyzed [28]. Data were analyzed using LightCycler Analysis Software 3.5.3 (Roche Diagnostics).

### *Statistical Analysis*

Values are presented as mean ± SD. The Mann-Whitney $U$ test was used for comparison between groups. $P < .05$ was considered significant. Statistical analysis was performed using the statistical software SPSS 16.0 (SPSS, Inc., Chicago, IL).

## Results

### *PEDF-Transfected Rat Tumor Cells Secreted Biologically Active PEDF*

To study the effects of PEDF on prostate tumor growth and metastasis, we transfected rat MatLyLu prostate tumor cells, a metastatic

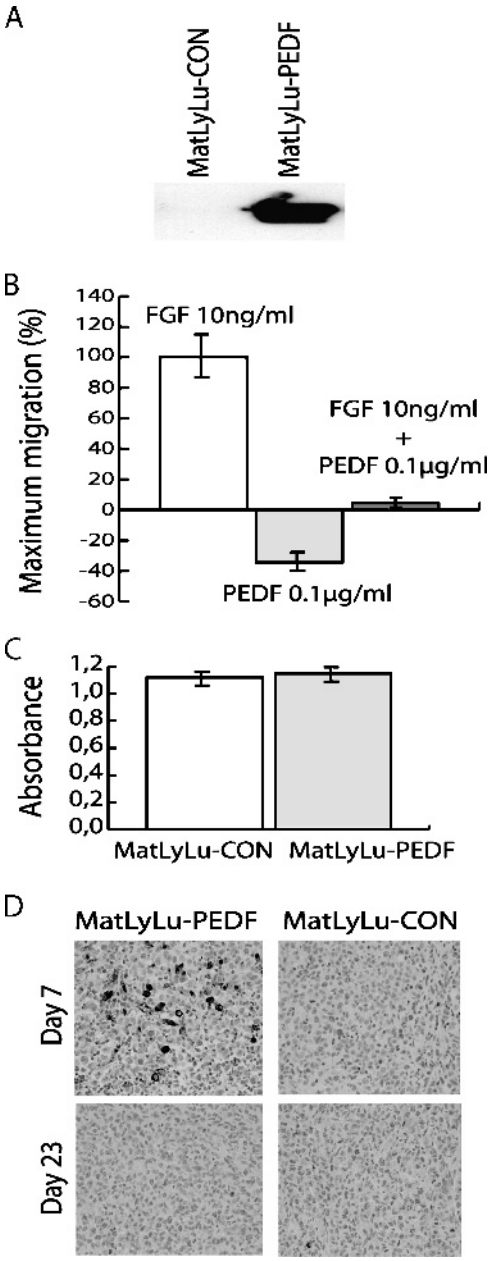


**Figure 1.** (A) Western blot analysis of PEDF in PEDF-transfected (MatLyLu-PEDF) and vector-transfected MatLyLu (MatLyLu-CON) cells *in vitro*. (B) PEDF purified from MatLyLu-PEDF medium was tested for its ability to inhibit migration of HUVECs toward angiogenic FGF2. Results are presented as percentage maximum migration induced by the positive control (FGF2) after the background migration of endothelial cells was subtracted. (C) Cell viability was measured in MatLyLu-PEDF and control cells after 72 hours using an MTT assay. (D) Sections from orthotopic MatLyLu-PEDF and MatLyLu-CON tumors immunostained with an antibody against human PEDF (Chemicon).

cell type that normally lacks PEDF expression [28], with a plasmid vector containing human PEDF cDNA (MatLyLu-PEDF). Control cells were transfected with the same vector lacking PEDF cDNA (MatLyLu-CON). PEDF was detected in conditioned medium of MatLyLu-PEDF cells, whereas the conditioned medium of control cells was negative (Figure 1*A*). Purified PEDF protein from MatLyLu-PEDF conditioned medium inhibited HUVEC migration above the basal levels (Figure 1*B*) in line with effects reported earlier for recombinant PEDF [15]. These results show that the PEDF protein was synthesized, secreted, and biologically active. However, viability did not differ between PEDF-transfected and control cells, indicating that PEDF overexpression did not have strong effects on the MatLyLu cells *in vitro* (Figure 1*C*).

### *PEDF Overexpression Slowed Orthotopic Prostate Tumor Growth, Inhibited Angiogenesis, and Repressed the Growth of Lymph Node Metastasis*

To evaluate the growth rate of MatLyLu-PEDF cells *in vivo*, a small number of cells ($1 \times 10^4$) were injected into the ventral prostate of Copenhagen rats and compared with controls at 7 and 23 days after injection.

Tumor size was significantly smaller in the MatLyLu-PEDF tumors compared with controls at both time points (Table 1). However, tumor growth between days 7 and 23 was high in both MatLyLu-PEDF tumors and controls and was probably due to transient PEDF expression *in vivo*. At day 7, human PEDF mRNA (data not shown) and protein was expressed in MatLyLu-PEDF tumors, whereas MatLyLu-CON tumors were negative. Immunohistochemistry at day 7 showed that some tumor cells where highly immunoreactive for PEDF, whereas others were completely unstained, and at 23 days, the protein expression was no longer detected (Figure 1*D*). The transient expression of PEDF expression was probably due to loss of the expression plasmid during tumor expansion, and we, therefore, further analyzed the tumors at day 7 when PEDF protein was present.

Histologic analysis at day 7 showed that PEDF inhibited angiogenesis in the MatLyLu-tumors and in the nearby normal prostate tissue (Table 1). Surprisingly, MatLyLu-PEDF tumors contained more lymphatic vessel in the tumor adjacent prostate tissue compared with controls (Table 1). Further, PEDF did not affect tumor cell proliferation, and although tumor cell apoptosis was increased, it did not reach statistical significance, indicating that tumor growth was inhibited during earlier time points. Previous studies have shown that PEDF could suppress prostate tumor growth by inducing neuroendocrine differentiation [27]. We could, however, not detect any neuroendocrine marker expression (synaptophysin) or phenotype in MatLyLu-PEDF tumors (data not shown).

Examination of abdominal lymph node and lung tissue showed no signs of metastasis at the earlier time point. At day 23, abdominal

**Table 1.** Histologic Analysis of MatLyLu-PEDF and Control Tumors.

| | MatLyLu-CON | MatLyLu-PEDF | *P* |
|---|---|---|---|
| MatLyLu-PEDF (*n* = *8*) and control tumors (*n* = *7*) at day 7 | | | |
| Tumor weight (g) | 0.045 (0.024) | 0.015 (0.013) | .02 |
| Vascular density (intratumoral) factor VIII (%) | 4.7 (0.7) | 2.6 (1.2) | .008 |
| Vascular density (extratumoral) factor VIII (%) | 4.3 (1.0) | 2.6 (0.9) | .005 |
| Lymphatic vessel density (extratumoral) LYVE-1 (%) | 0.5 (0.1) | 0.8 (0.2) | .009 |
| Apoptosis caspase-3 (%) | 1.2 (0.5) | 1.8 (0.6) | .08 |
| Proliferation BrdU (%) | 26.3 (3.4) | 22.0 (6.5) | .2 |
| MatLyLu-PEDF (*n* = *11*) and control tumors (*n* = *9*) at day 23 | | | |
| Tumor weight (g) | 28 (9.0) | 19 (7.4) | .04 |
| Lymph node metastasis (mm) | 3.7 (2.0) | 1.1 (1.0) | .005 |

Values are means (SD).

lymph node metastases were seen in all nine control animals, and in addition, metastases to lungs and/or liver were detected in three of nine MatLyLu-CON animals. In the MatLyLu-PEDF group, lymph node metastases were seen in 8 of 11 examined animals, but the average diameter of the metastases was significantly reduced compared with controls (Table 1). Metastases to the lung and/or liver were only seen in 1 of the 11 PEDF transfected animals. Transient overexpression of PEDF was thus sufficient to temporarily inhibit growth of prostate tumors and their metastases.

### *PEDF Transfection Influenced the Expression of Vascular Regulators and Cytokines in Prostate Cancer Cells*

To better understand the mechanisms behind PEDF's antiangiogenic effects and to study if PEDF induced chemokine's expressions, MatLyLu-PEDF cells were compared with control cells using a rat chemokine and a rat angiogenesis PCR array. The results showed that PEDF expression induced MatLyLu cells *in vitro* to express other antiangiogenic factors such as bone morphogenetic protein 6 (Bmp6) [39], tissue inhibitor of metalloproteinase 2 [40], midkine [41], and the metastasis suppressor maspin [42] (Table 2). However, proangiogenic factors, for example, FGF2, matrix metalloproteinase 9 (MMP9), placental growth factor (PlGF), and ephrin A1, were also increased [43] (Table 2). As the tumor *in vivo* showed decreased angiogenesis, these observations emphasize the importance of the net balance of proangiogenic and antiangiogenic molecules.

MatLyLu-PEDF tumor cells also had increased expression of several chemokines *in vitro* compared with MatLyLu-CON cells (Table 2). A subset of these has been shown to stimulate infiltration of macrophages in other tissues, for example, chemokines ligand 6 (CCL6) [44] and PlGF [45]. The recruitment factors MCP-1/CCL2 and colony-stimulating factor 1 were, however, not increased in the MatLyLu-PEDF tumor cells compared with controls.

### *PEDF Overexpression Increased Tumor Macrophage Recruitment* In Vivo

To examine if PEDF overexpression could influence monocyte/macrophage infiltration, we stained the tumors for CD68 (Figure 2*A*). Surprisingly, MatLyLu-PEDF tumors and their surrounding prostate tissue contained significantly more macrophages than MatLyLu-CON tumors (Figure 2*B*).

TAMs are present in most established tumors and differentiate into cytotoxic (M1) macrophages but more generally to the tumor growth-promoting (M2) state [4]. Increased iNOS is a characteristic of M1 macrophages [46]. To compare iNOS expression *in vivo*, we stained MatLyLu-PEDF tumors and controls using an iNOS antibody (Figure 2*A*). The volume density of iNOS-positive macrophages increased in the MatLyLu-PEDF tumors compared with controls both in the nonmalignant tissue and in the tumor (Figure 2*C*). More than half of the TAMs in the extratumoral nonmalignant tissue were iNOS-positive in both MatLyLu-PEDF tumors and controls (Figure 2*D*). Inside the tumor, the fraction of iNOS-positive macrophages was lower compared with the extratumoral tissue, suggesting a shift in the macrophage phenotype in the tumor microenvironment. Furthermore, the data show that, although iNOS-positive macrophages are a minor fraction of the TAMs inside the MatLyLu tumors, their proportion increased when the tumors overexpressed PEDF (Figure 2*D*).

**Table 2.** Chemokines and Angiogenic Factors Altered in MatLyLu-PEDF Cells Compared with MatLyLu-CON Cells *In Vitro* (Two-fold Cutoff).

| Accession No. | Symbol | Description | Fold Change in Superarray |
|---|---|---|---|
| Angiogenic factors | | | |
| NM_031530 | *CCL2/MCP-1* | Chemokine (C-C) ligand 2 | −3.30 |
| XM_343607 | *Col4a3* | Collagen, type IV, α 3 | −2.24 |
| NM_145672 | *CXCL9/Mig* | Chemokine (C-X-C) ligand 9 | −3.37 |
| NM_053599 | *Efna1* | Ephrin A1 | 2.77 |
| NM_001010968 | *Eng* | Endoglin | 3.44 |
| NM_022924 | *F2* | Coagulation factor 2 | 2.79 |
| NM_019305 | *Fgf-2/bFGF* | Fibroblast growth factor 2 | 2.22 |
| NM_131908 | *Fgf-6* | Fibroblast growth factor 6 | 2.11 |
| NM_019143 | *Fn-1* | Fibronectin 1 | 2.27 |
| NM_024359 | *Hif1α* | Hypoxia-inducible factor 1 α | 2.91 |
| NM_012589 | *IL6* | Interleukin 6 | 2.92 |
| XM_215963 | *Lama5* | Laminin, α 5 | 3.41 |
| NM_030854 | *Lect1* | Leukocyte cell derived chemotaxin 1 | −2.38 |
| NM_030859 | *Mdk* | Midkine | 6.19 |
| NM_031055 | *Mmp9* | Matrix metalloproteinase 9 | 7.82 |
| U77697 | *Pecam* | Platelet/endothelial cell adhesion molecule | 2.60 |
| NM_053595 | *Plgf* | Placental growth factor | 2.03 |
| NM_057108 | *Serpinb5* | Maspin | 2.73 |
| NM_012671 | *TGFα* | Transforming growth factor α | 3.00 |
| NM_021578 | *TGFβ2* | Transforming growth factor β 2 | 2.54 |
| NM_013174 | *TGFβ3* | Transforming growth factor β 3 | 2.08 |
| NM_053819 | *Timp-2* | Tissue inhibitor of metalloproteinase 2 | 2.72 |
| Chemokines | | | |
| NM_011349 | *Agtrl1* | Angiotensin receptor-like 1 | 2.93 |
| NM_013107 | *Bmp6* | Bone morphogenetic protein 6 | 2.93 |
| NM_016994 | *C3* | Complement component 3 | 3.96 |
| NM_078621 | *Ccbp2* | Chemokine binding protein 2 | 2.15 |
| NM_057151 | *Ccl17* | Chemokine (C-C motif) ligand 17 | 3.84 |
| NM_0010042 | *Ccl6* | Chemokine (C-C motif) ligand 6 | 17.17 |
| NM_0010123 | *Ccl9* | Chemokine (C-C motif) ligand 9 | 3.38 |
| NM_020542 | *Ccr1* | Chemokine (C-C motif)receptor 1 | −9.18 |
| NM_133532 | *Ccr4* | Chemokine (C-C motif) receptor 4 | 2.15 |
| NM_0010131 | *Ccr6* | Chemokine (C-C motif) receptor 6 | 2.22 |
| NM_172329 | *Ccr9* | Chemokine (C-C motif)receptor 9 | 5.48 |
| NM_022218 | *Cmklr1* | Chemokine-like receptor 1 | 5.30 |
| NM_053352 | *Cmkor1* | Chemokine orphan receptor 1 | 5.98 |
| NM_182952 | *Cxc111* | Chemokine (C-X-C motif) ligand 11 | 4.14 |
| NM_053647 | *Cxcl2* | Chemokine (C-X-C motif) ligand 2 | 3.96 |
| NM_017001 | *Epo* | Erythropoietin | 5.28 |
| XM_344130 | *Inhbb* | Inhibin β-B | 5.66 |
| NM_022196 | *Lif* | Leukemia inhibitory factor | 2.17 |
| NM_019340 | *Rgs3* | Regulator of G protein signaling 3 | 2.08 |
| NM_019178 | *Tlr4* | Toll-like receptor 4 | 24.93 |

### *PEDF Levels in Prostate Tumors Were Suppressed by the Microenvironment and TNFα*

Because prostate tumors and tumor cell lines often, and for reasons unknown, lack PEDF expression [26,28], it was of interest to explore how PEDF was regulated in the prostate and in prostate tumors.

To start exploring this, we first examined how prostate tumor cells normally expressing PEDF behave when placed in a prostate microenvironment. AT-1 tumor cells that express high levels of PEDF mRNA and protein *in vitro* and as subcutaneous tumors [28] were injected into the ventral prostate of Copenhagen rats. Interestingly, PEDF mRNA and protein levels were downregulated in AT-1 tumors growing in the prostate compared with the tumor cells *in vitro* (Figure 3, *A* and *B*), suggesting that some factor in the prostate microenvironment suppressed the PEDF intratumoral system. To ensure that equal levels of RNA were analyzed, GAPDH mRNA levels were quantified. No significant difference in the GAPDH mRNA levels was observed (data not shown).

In previous studies, we have shown that intraprostatic injection of AT-1 cells results in the accumulation of inflammatory cells such

as macrophages and mast cells in the tumor and in the surrounding normal tissue [8] (Johansson et al., unpublished data). It is therefore possible that factors secreted by inflammatory cells downregulate endogenous PEDF expression possibly as a negative feedback loop. Immunohistochemical staining showed that inflammatory cells, mainly macrophages, were positively stained for TNFα, whereas AT-1 tumor cells were negative (Figure 3*C*). TNFα stimulation of AT-1 cells *in vitro* significantly decreased PEDF mRNA levels in a dose-dependent manner (Figure 3*D*). GAPDH mRNA levels were unaffected, and TNFα did not affect cell viability after the 18-hour incubation (data not shown). In addition, TNFα decreased PEDF protein in conditioned medium of AT-1 cells (Figure 3*E*). To test if TNFα could regulate the expression of PEDF *in vivo*, a single dose of TNFα (1 μg per animal) was injected into the ventral prostate of Copenhagen rats, and the animals were killed 6 hours later. The results showed that TNFα significantly downregulated PEDF mRNA also in normal rat prostate tissue *in vivo* (Figure 3*F*). GAPDH mRNA expression did not differ significantly between the groups (data not shown).

## Discussion

MatLyLu rat prostate tumors are highly aggressive and metastatic and express low levels of PEDF *in vivo* and *in vitro* [28]. Here, we transiently transfected MatLyLu tumor cells with a plasmid vector expressing human PEDF. Consistent with studies in other cancer types [16–22], PEDF overexpression also repressed orthotopic MatLyLu tumor growth, delayed the growth of metastasis, and suppressed angiogenesis both in the tumor and in the surrounding normal prostate. The antiangiogenic effects seen in this model could be due to direct inhibitory effects of PEDF on blood vessels or indirect effects caused by other factors upregulated by PEDF. For example, angiogenesis inhibitors such as maspin [42], midkine [41], and Bmp6 [39] were upregulated, but stimulators such as MMP9, FGF2, and PlGF were also upregulated. Exploiting the antiangiogenic effects of PEDF could thus be a novel way to treat prostate cancer, but our findings suggest that PEDF also has additional functions.

Interestingly, we also found that PEDF-transfected tumors contained more macrophages both in the tumor and in the adjacent prostate tissue than controls. Whether increased macrophage recruitment inhibits

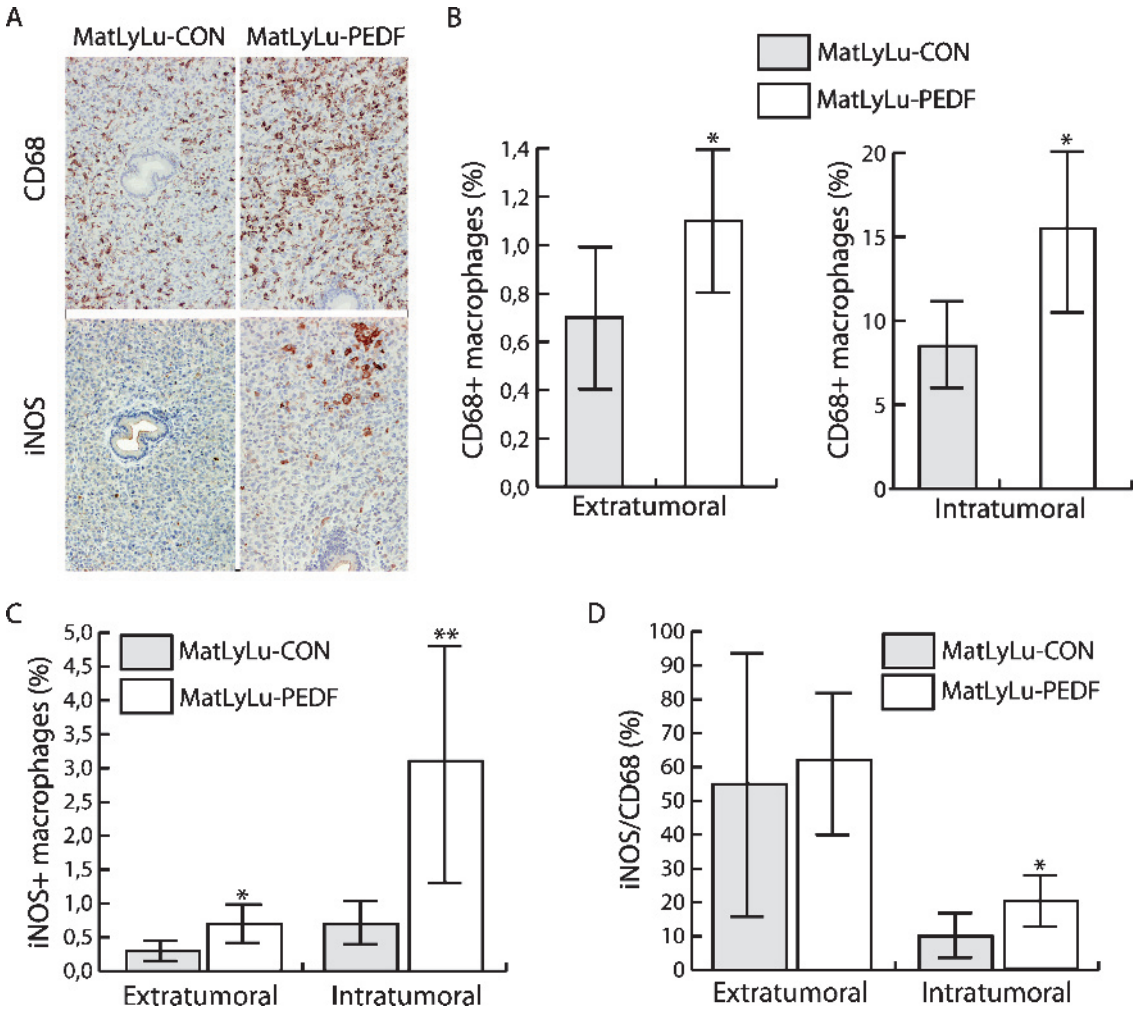


**Figure 2.** (A) Sections from MatLyLu-PEDF tumors and controls at day 7 showing consecutive areas stained for CD68 and iNOS-positive macrophages. (B) Volume densities (%) of CD68-positive macrophages and (C) iNOS-positive macrophages in the nonmalignant extratumoral tissue and intratumorally in MatLyLu-PEDF tumors and controls at day 7. (D) Percentage of iNOS-positive macrophages (iNOS/CD68) in the extratumoral and intratumoral tissues of MatLyLu-PEDF tumors and controls at day 7. Values are expressed as means ± SD. **P* < .05, ***P* < .01.

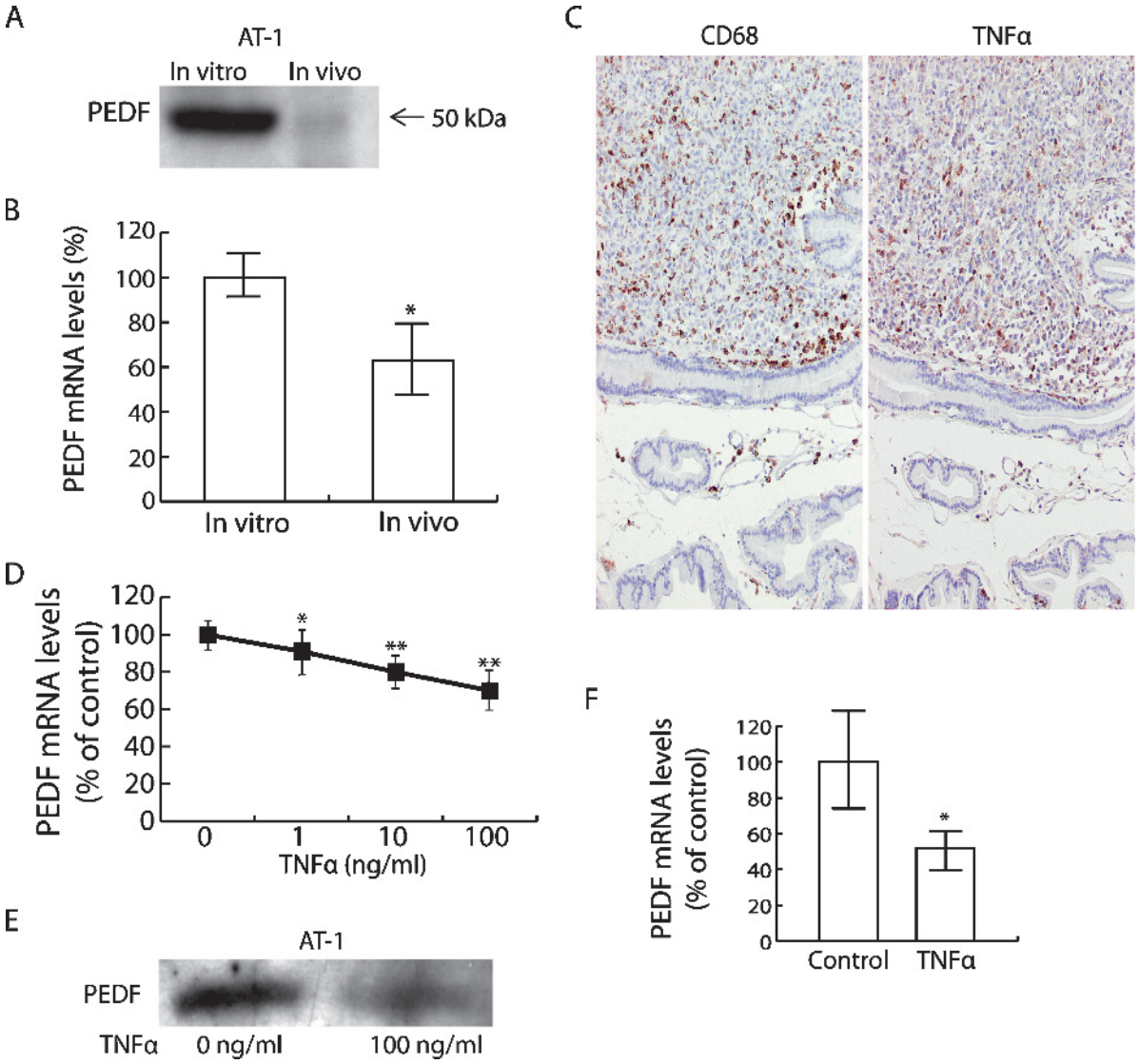


**Figure 3.** (A) Western blot analysis of PEDF in conditioned medium of AT-1 cells *in vitro* and in tumor lysates from orthotopic AT-1 tumors at day 10. (B) Relative PEDF mRNA levels in AT-1 cells *in vitro* ($n = 3$ different batches) and in orthotopic AT-1 tumors *in vivo* at day 10 ($n = 5$). (C) Sections from an AT-1 tumor at day 10 showing consecutive areas stained for macrophages (CD68) and TNFα. (D) Relative PEDF mRNA expression in AT-1 cells stimulated with indicated concentrations of TNFα for 18 hours *in vitro*. (E) Western blot analysis of PEDF in conditioned medium of AT-1 cells stimulated with indicated concentrations of TNFα for 24 hours. (F) Relative PEDF mRNA levels quantified from ventral prostate of Copenhagen rats injected with control (PBS, $n = 5$) or recombinant rat TNFα (1 μg, $n = 5$). Values are means ± SD. $^*P < .05$, $^{**}P < .01$.

or enhances tumor growth depends on their differentiation state, cytotoxic M1 macrophages inhibit tumor growth, whereas M2 macrophages are tumor promoting [3,4]. The tumor microenvironment generally directs macrophages toward the tumor-promoting phenotype, and we have previously shown that an overall reduction of monocyte/macrophage recruitment to rat AT-1 prostate tumors represses tumor growth and angiogenesis [8]. Here, we could demonstrate that the proportion of iNOS-positive macrophages (most likely M1) decreased inside the orthotopic MatLyLu tumor compared with the extratumoral nonmalignant prostate tissue, suggesting a shift in macrophage differentiation in the tumor microenvironment. Although iNOS-positive macrophages constituted a minor fraction of the total macrophage density in the MatLyLu tumors, the proportion was increased when the tumors overexpressed PEDF. This suggests that PEDF, in addition to its antiangiogenic functions, could also enhance antitumor immunity by increasing M1 macrophage numbers. Increased macrophage infiltration coupled with a shift from M2 to M1 macrophages by GM–colony-stimulating factor treatment has been shown to suppress breast cancer growth, angiogenesis, and metastasis [47]. Interestingly, another potent angiogenesis inhibitor, thrombospondin 1, has also been shown to promote M1 tumor macrophage recruitment and cytotoxicity [48].

The reason for the increased macrophage content is unknown, but PEDF has, in other tissues, been shown to either stimulate or repress the expression of several chemokines such as MCP-1/CCL2, macrophage inflammatory protein 1α, 2, and 3α, interleukin 1β, interleukin 6, and TNFα [9,10,13,49]. In this study, PEDF stimulated the expression of several chemokines and other factors in the MatLyLu tumor cells *in vitro*, which could directly or indirectly, through other

immune cells, result in macrophage recruitment [45,50]. CCL6, which attracts macrophages in rodents [44], was particularly upregulated, suggesting that it could be involved. Interestingly, Toll-like receptor 4 (TLR4) mRNA expression was highly increased in MatLyLu-PEDF cells compared with controls, and down-regulation of TLR4 signaling makes prostate cancer cells less aggressive [51]. Activation of TLR4 induces expression of several chemokines [52,53]. PEDF could therefore indirectly stimulate monocyte recruitment and make tumor cells more malignant by upregulating TLR4.

The possibility that increased macrophage accumulation to the MatLyLu-PEDF tumors also could be stimulatory is supported by the increase in lymphangiogenesis seen in the extratumoral prostate tissue. Lymphatic endothelial migration and survival is mainly stimulated by activation of vascular endothelial growth factor receptor 3 (VEGF-R3) by VEGF-C and D [54]. PEDF has been shown to stimulate both VEGF-C and VEGF-R3 expressions in endothelial HUVECs under hypoxia [55]. Here, in normoxic conditions *in vitro*, no difference in MatLyLu VEGF-C or VEGF-D mRNA levels could be detected. Because MatLyLu tumors are hypoxic *in vivo* (unpublished data), PEDF could possibly stimulate VEGF-C expression in this context. Macrophages are, however, by secreting VEGF-C and VEGF-D, potent stimulators of peritumoral lymphangiogenesis [56]. Therefore, PEDF could, indirectly by stimulating macrophage infiltration to the tumors, stimulate lymphangiogenesis. Because lymphangiogenesis could enhance the metastatic potential of tumors [57], these findings are contradictory to PEDF as a clean metastasis suppressor and therefore warrant further investigations.

PEDF expression is often decreased or lost in prostate tumors and prostate tumor cell lines [26,28]. The reason for this is unknown, but hypoxia and androgens can downregulate PEDF protein in prostate stromal and tumor cells [26]. In our previous work, we could find subsets of aggressive human prostate tumors that still contained PEDF; however, immunohistochemistry showed that the expression of PEDF was heterogeneous [28]. Orgaz et al. [33] showed that a single melanoma lesion may contain both PEDF-positive and -negative cells and that PEDF expression was restricted to the less aggressive tumor cells. Regulatory signals from the microenvironment may provide a mechanism underlying such changes in PEDF expression. This was supported by our results showing that injection of AT-1 tumor cells into the prostate of Copenhagen rats markedly decreased the expression of endogenous PEDF compared with the levels *in vitro*. AT-1 tumor cells placed subcutaneously, however, did not decrease PEDF expression [28] (unpublished data), suggesting that some factor in the prostate microenvironment inhibited PEDF expression. Our AT-1 tumors are hypoxic [35], and hypoxia is therefore one likely explanation for the decreased levels of PEDF in the orthotopic tumors compared with the tumor cells *in vitro*. Hypoxia-induced down-regulation has, however, only been seen at the translational/posttranslation level and not at the transcriptional level [15], but in the AT-1 tumors, both mRNA and protein were markedly reduced. Furthermore, androgens should not affect the AT-1 tumors because they lack the androgen receptor [35,58]. This prompted us to look for additional regulatory mechanisms for PEDF. Macrophages and other inflammatory cells such as T cells and mast cells accumulate in the AT-1 tumors and in the surrounding normal tissue [8] (Johansson et al., unpublished data). We could show that these inflammatory cells, mainly macrophages but also other inflammatory cells, express TNFα and that TNFα downregulated PEDF expression in AT-1 cells *in vitro* and in the ventral prostate *in vivo*. These results suggest that tumor infiltration by TNFα-expressing macrophages could eventually facilitate angiogenesis, tumor growth, and metastasis by repressing PEDF expression in prostate tumor cells. As PEDF overexpression stimulated increased macrophage infiltration to MatLyLu tumors, it is possible that TNFα secreted by macrophages could work as a negative feedback loop for PEDF expression. Loss of PEDF overexpression in the MatLyLu tumors is, however, probably due to loss of the expression plasmid during tumor growth. TNFα has also been shown to decrease PEDF mRNA in HUVECs [59]. Interestingly, accumulating immune cells secreting RANK-ligand affecting NFκB signaling in prostate tumor cells have also been shown to inhibit the secretion of another metastasis inhibiting serpin maspin [60], which was upregulated *in vitro* by PEDF overexpression in our study. Infiltrating macrophages may thus enhance prostate tumor progression by downregulating endogenous antiangiogenic and metastasis-suppressing factors.

PEDF is a potent tumor suppressor and is therefore a promising anticancer therapy. Here, we also show that PEDF, besides inhibiting angiogenesis, also increased the fraction of iNOS-positive and most likely cytotoxic macrophages to prostate tumors, suggesting an additional antitumor function. Accumulating macrophages may, however, by secreting TNFα and other factors, suppress the secretion of PEDF and other inhibitors of angiogenesis and promote lymphangiogenesis and, in this way, facilitate tumor progression. PEDF treatment could therefore be a double-edged sword, and to clarify its potential use in treatment, the multiple functions of this protein need to be thoroughly investigated.

## Acknowledgment

The authors thank Sigrid Kilter, Pernilla Andersson, Elisabeth Dahlberg, and Birgitta Ekblom for their skillful technical assistance.

## References

[1] Witz IP (2009). The tumor microenvironment: the making of a paradigm. *Cancer Microenviron* **2** (Suppl 1), 9–17.

[2] Pollard JW (2004). Tumour-educated macrophages promote tumour progression and metastasis. *Nat Rev Cancer* **4**, 71–78.

[3] Biswas SK, Sica A, and Lewis CE (2008). Plasticity of macrophage function during tumor progression: regulation by distinct molecular mechanisms. *J Immunol* **180**, 2011–2017.

[4] Sica A, Larghi P, Mancino A, Rubino L, Porta C, Totaro MG, Rimoldi M, Biswas SK, Allavena P, and Mantovani A (2008). Macrophage polarization in tumour progression. *Semin Cancer Biol* **18**, 349–355.

[5] Lissbrant IF, Stattin P, Wikstrom P, Damber JE, Egevad L, and Bergh A (2000). Tumor associated macrophages in human prostate cancer: relation to clinicopathological variables and survival. *Int J Oncol* **17**, 445–451.

[6] Shimura S, Yang G, Ebara S, Wheeler TM, Frolov A, and Thompson TC (2000). Reduced infiltration of tumor-associated macrophages in human prostate cancer: association with cancer progression. *Cancer Res* **60**, 5857–5861.

[7] Loberg RD, Ying C, Craig M, Yan L, Snyder LA, and Pienta KJ (2007). CCL2 as an important mediator of prostate cancer growth *in vivo* through the regulation of macrophage infiltration. *Neoplasia* **9**, 556–562.

[8] Halin S, Rudolfsson SH, Van Rooijen N, and Bergh A (2009). Extratumoral macrophages promote tumor and vascular growth in an orthotopic rat prostate tumor model. *Neoplasia* **11**, 177–186.

[9] Sanagi T, Yabe T, and Yamada H (2005). The regulation of pro-inflammatory gene expression induced by pigment epithelium–derived factor in rat cultured microglial cells. *Neurosci Lett* **380**, 105–110.

[10] Takanohashi A, Yabe T, and Schwartz JP (2005). Pigment epithelium–derived factor induces the production of chemokines by rat microglia. *Glia* **51**, 266–278.

[11] Wang JJ, Zhang SX, Mott R, Chen Y, Knapp RR, Cao W, and Ma JX (2008). Anti-inflammatory effects of pigment epithelium–derived factor in diabetic nephropathy. *Am J Physiol Renal Physiol* **294**, F1166–F1173.

[12] Zamiri P, Masli S, Streilein JW, and Taylor AW (2006). Pigment epithelial growth factor suppresses inflammation by modulating macrophage activation. *Invest Ophthalmol Vis Sci* **47**, 3912–3918.
[13] Zhang SX, Wang JJ, Gao G, Shao C, Mott R, and Ma JX (2006). Pigment epithelium–derived factor (PEDF) is an endogenous antiinflammatory factor. *FASEB J* **20**, 323–325.
[14] Tombran-Tink J (2005). The neuroprotective and angiogenesis inhibitory serpin, PEDF: new insights into phylogeny, function, and signaling. *Front Biosci* **10**, 2131–2149.
[15] Dawson DW, Volpert OV, Gillis P, Crawford SE, Xu H, Benedict W, and Bouck NP (1999). Pigment epithelium–derived factor: a potent inhibitor of angiogenesis. *Science* **285**, 245–248.
[16] Abe R, Shimizu T, Yamagishi S, Shibaki A, Amano S, Inagaki Y, Watanabe H, Sugawara H, Nakamura H, Takeuchi M, et al. (2004). Overexpression of pigment epithelium–derived factor decreases angiogenesis and inhibits the growth of human malignant melanoma cells *in vivo*. *Am J Pathol* **164**, 1225–1232.
[17] Garcia M, Fernandez-Garcia NI, Rivas V, Carretero M, Escamez MJ, Gonzalez-Martin A, Medrano EE, Volpert O, Jorcano JL, Jimenez B, et al. (2004). Inhibition of xenografted human melanoma growth and prevention of metastasis development by dual antiangiogenic/antitumor activities of pigment epithelium–derived factor. *Cancer Res* **64**, 5632–5642.
[18] Ek ET, Dass CR, Contreras KG, and Choong PF (2007). Pigment epithelium–derived factor overexpression inhibits orthotopic osteosarcoma growth, angiogenesis and metastasis. *Cancer Gene Ther* **14**, 616–626.
[19] Crawford SE, Stellmach V, Ranalli M, Huang X, Huang L, Volpert O, De Vries GH, Abramson LP, and Bouck N (2001). Pigment epithelium–derived factor (PEDF) in neuroblastoma: a multifunctional mediator of Schwann cell antitumor activity. *J Cell Sci* **114**, 4421–4428.
[20] Streck CJ, Zhang Y, Zhou J, Ng C, Nathwani AC, and Davidoff AM (2005). Adeno-associated virus vector–mediated delivery of pigment epithelium–derived factor restricts neuroblastoma angiogenesis and growth. *J Pediatr Surg* **40**, 236–243.
[21] Abramson LP, Stellmach V, Doll JA, Cornwell M, Arensman RM, and Crawford SE (2003). Wilms' tumor growth is suppressed by antiangiogenic pigment epithelium–derived factor in a xenograft model. *J Pediatr Surg* **38**, 336–342; discussion 336–342.
[22] Mahtabifard A, Merritt RE, Yamada RE, Crystal RG, and Korst RJ (2003). *In vivo* gene transfer of pigment epithelium–derived factor inhibits tumor growth in syngeneic murine models of thoracic malignancies. *J Thorac Cardiovasc Surg* **126**, 28–38.
[23] Fernandez-Garcia NI, Volpert OV, and Jimenez B (2007). Pigment epithelium–derived factor as a multifunctional antitumor factor. *J Mol Med* **85**, 15–22.
[24] Filleur S, Nelius T, de Riese W, and Kennedy RC (2009). Characterization of PEDF: a multi-functional serpin family protein. *J Cell Biochem* **106**, 769–775.
[25] Ek ET, Dass CR, and Choong PF (2006). PEDF: a potential molecular therapeutic target with multiple anti-cancer activities. *Trends Mol Med* **12**, 497–502.
[26] Doll JA, Stellmach VM, Bouck NP, Bergh AR, Lee C, Abramson LP, Cornwell ML, Pins MR, Borensztajn J, and Crawford SE (2003). Pigment epithelium–derived factor regulates the vasculature and mass of the prostate and pancreas. *Nat Med* **9**, 774–780.
[27] Filleur S, Volz K, Nelius T, Mirochnik Y, Huang H, Zaichuk TA, Aymerich MS, Becerra SP, Yap R, Veliceasa D, et al. (2005). Two functional epitopes of pigment epithelial–derived factor block angiogenesis and induce differentiation in prostate cancer. *Cancer Res* **65**, 5144–5152.
[28] Halin S, Wikstrom P, Rudolfsson SH, Stattin P, Doll JA, Crawford SE, and Bergh A (2004). Decreased pigment epithelium–derived factor is associated with metastatic phenotype in human and rat prostate tumors. *Cancer Res* **64**, 5664–5671.
[29] Cai J, Parr C, Watkins G, Jiang WG, and Boulton M (2006). Decreased pigment epithelium–derived factor expression in human breast cancer progression. *Clin Cancer Res* **12**, 3510–3517.
[30] Zhang L, Chen J, Ke Y, Mansel RE, and Jiang WG (2006). Expression of pigment epithelial derived factor is reduced in non–small cell lung cancer and is linked to clinical outcome. *Int J Mol Med* **17**, 937–944.
[31] Uehara H, Miyamoto M, Kato K, Ebihara Y, Kaneko H, Hashimoto H, Murakami Y, Hase R, Takahashi R, Mega S, et al. (2004). Expression of pigment epithelium–derived factor decreases liver metastasis and correlates with favorable prognosis for patients with ductal pancreatic adenocarcinoma. *Cancer Res* **64**, 3533–3537.
[32] Guan M, Yam HF, Su B, Chan KP, Pang CP, Liu WW, Zhang WZ, and Lu Y (2003). Loss of pigment epithelium derived factor expression in glioma progression. *J Clin Pathol* **56**, 277–282.
[33] Orgaz JL, Ladhani O, Hoek KS, Fernandez-Barral A, Mihic D, Aguilera O, Seftor EA, Bernad A, Rodriguez-Peralto JL, Hendrix MJ, et al. (2009). Loss of pigment epithelium–derived factor enables migration, invasion and metastatic spread of human melanoma. *Oncogene* **28**, 4147–4161.
[34] Sidle DM, Maddalozzo J, Meier JD, Cornwell M, Stellmach V, and Crawford SE (2005). Altered pigment epithelium–derived factor and vascular endothelial growth factor levels in lymphangioma pathogenesis and clinical recurrence. *Arch Otolaryngol Head Neck Surg* **131**, 990–995.
[35] Halin S, Hammarsten P, Wikstrom P, and Bergh A (2007). Androgen-insensitive prostate cancer cells transiently respond to castration treatment when growing in an androgen-dependent prostate environment. *Prostate* **67**, 370–377.
[36] Franck-Lissbrant I, Haggstrom S, Damber JE, and Bergh A (1998). Testosterone stimulates angiogenesis and vascular regrowth in the ventral prostate in castrated adult rats. *Endocrinology* **139**, 451–456.
[37] Johansson A, Rudolfsson SH, Wikstrom P, and Bergh A (2005). Altered levels of angiopoietin 1 and tie 2 are associated with androgen-regulated vascular regression and growth in the ventral prostate in adult mice and rats. *Endocrinology* **146**, 3463–3470.
[38] Lissbrant IF, Hammarsten P, Lissbrant E, Ferrara N, Rudolfsson SH, and Bergh A (2004). Neutralizing VEGF bioactivity with a soluble chimeric VEGF-receptor protein flt(1-3)IgG inhibits testosterone-stimulated prostate growth in castrated mice. *Prostate* **58**, 57–65.
[39] Seckinger A, Meissner T, Moreaux J, Goldschmidt H, Fuhler GM, Benner A, Hundemer M, Reme T, Shaughnessy JD Jr, Barlogie B, et al. (2009). Bone morphogenic protein 6: a member of a novel class of prognostic factors expressed by normal and malignant plasma cells inhibiting proliferation and angiogenesis. *Oncogene* **28**, 3866–3879.
[40] Stetler-Stevenson WG (2008). The tumor microenvironment: regulation by MMP-independent effects of tissue inhibitor of metalloproteinases-2. *Cancer Metastasis Rev* **27**, 57–66.
[41] van der Horst EH, Frank BT, Chinn L, Coxon A, Li S, Polesso F, Slavin A, Ruefli-Brasse A, and Wesche H (2008). The growth factor Midkine antagonizes VEGF signaling *in vitro* and *in vivo*. *Neoplasia* **10**, 340–347.
[42] Hall DC, Johnson-Pais TL, Grubbs B, Bernal R, Leach RJ, and Padalecki SS (2008). Maspin reduces prostate cancer metastasis to bone. *Urol Oncol* **26**, 652–658.
[43] Papetti M and Herman IM (2002). Mechanisms of normal and tumor-derived angiogenesis. *Am J Physiol Cell Physiol* **282**, C947–C970.
[44] LaFleur AM, Lukacs NW, Kunkel SL, and Matsukawa A (2004). Role of CC chemokine CCL6/C10 as a monocyte chemoattractant in a murine acute peritonitis. *Mediators Inflamm* **13**, 349–355.
[45] Coffelt SB, Hughes R, and Lewis CE (2009). Tumor-associated macrophages: effectors of angiogenesis and tumor progression. *Biochim Biophys Acta* **1796**, 11–18.
[46] Weigert A and Brune B (2008). Nitric oxide, apoptosis and macrophage polarization during tumor progression. *Nitric Oxide* **19**, 95–102.
[47] Eubank TD, Roberts RD, Khan M, Curry JM, Nuovo GJ, Kuppusamy P, and Marsh CB (2009). Granulocyte macrophage colony-stimulating factor inhibits breast cancer growth and metastasis by invoking an anti-angiogenic program in tumor-educated macrophages. *Cancer Res* **69**, 2133–2140.
[48] Martin-Manso G, Galli S, Ridnour LA, Tsokos M, Wink DA, and Roberts DD (2008). Thrombospondin 1 promotes tumor macrophage recruitment and enhances tumor cell cytotoxicity of differentiated U937 cells. *Cancer Res* **68**, 7090–7099.
[49] Yabe T, Sanagi T, Schwartz JP, and Yamada H (2005). Pigment epithelium–derived factor induces pro-inflammatory genes in neonatal astrocytes through activation of NF-κ B and CREB. *Glia* **50**, 223–234.
[50] Sica A, Allavena P, and Mantovani A (2008). Cancer related inflammation: the macrophage connection. *Cancer Lett* **267**, 204–215.
[51] Hua D, Liu MY, Cheng ZD, Qin XJ, Zhang HM, Chen Y, Qin GJ, Liang G, Li JN, Han XF, et al. (2009). Small interfering RNA-directed targeting of Toll-like receptor 4 inhibits human prostate cancer cell invasion, survival, and tumorigenicity. *Mol Immunol* **46**, 2876–2884.
[52] Chen R, Alvero AB, Silasi DA, Steffensen KD, and Mor G (2008). Cancers take their Toll—the function and regulation of Toll-like receptors in cancer cells. *Oncogene* **27**, 225–233.
[53] Sato Y, Goto Y, Narita N, and Hoon DS (2009). Cancer cells expressing Toll-like receptors and the tumor microenvironment. *Cancer Microenviron* **2** (Suppl 1), 205–214.

[54] Karpanen T and Alitalo K (2008). Molecular biology and pathology of lymphangiogenesis. *Annu Rev Pathol* **3**, 367–397.

[55] Aparicio S, Sawant S, Lara N, Barnstable CJ, and Tombran-Tink J (2005). Expression of angiogenesis factors in human umbilical vein endothelial cells and their regulation by PEDF. *Biochem Biophys Res Commun* **326**, 387–394.

[56] Schoppmann SF, Birner P, Stockl J, Kalt R, Ullrich R, Caucig C, Kriehuber E, Nagy K, Alitalo K, and Kerjaschki D (2002). Tumor-associated macrophages express lymphatic endothelial growth factors and are related to peritumoral lymphangiogenesis. *Am J Pathol* **161**, 947–956.

[57] Stacker SA, Baldwin ME, and Achen MG (2002). The role of tumor lymphangiogenesis in metastatic spread. *FASEB J* **16**, 922–934.

[58] Isaacs JT, Isaacs WB, Feitz WF, and Scheres J (1986). Establishment and characterization of seven Dunning rat prostatic cancer cell lines and their use in developing methods for predicting metastatic abilities of prostatic cancers. *Prostate* **9**, 261–281.

[59] Yamagishi S, Inagaki Y, Nakamura K, Abe R, Shimizu T, Yoshimura A, and Imaizumi T (2004). Pigment epithelium–derived factor inhibits TNF-α–induced interleukin-6 expression in endothelial cells by suppressing NADPH oxidase–mediated reactive oxygen species generation. *J Mol Cell Cardiol* **37**, 497–506.

[60] Luo JL, Tan W, Ricono JM, Korchynskyi O, Zhang M, Gonias SL, Cheresh DA, and Karin M (2007). Nuclear cytokine–activated IKKα controls prostate cancer metastasis by repressing Maspin. *Nature* **446**, 690–694.